Thermodynamic stability, compressibility matrices, and effects of mediated interactions in a strongly interacting Bose-Fermi mixture

Koki Manabe* and Yoji Ohashi
Department of Physics, Keio University, Yokohama 223-8522, Japan

(Received 31 March 2021; accepted 11 June 2021; published 23 June 2021)

We theoretically investigate the thermodynamic stability of a normal-state Bose-Fermi mixture, with a tunable Bose-Fermi pairing interaction $-U_{\rm BF} < 0$ associated with a heteronuclear Feshbach resonance, as well as a weak repulsive Bose-Bose interaction $U_{\rm BB} \geqslant 0$. Including strong heteropairing fluctuations associated with the former interaction within the self-consistent T-matrix approximation, as well as the latter within the mean-field level, we calculate the compressibility matrix, to assess the stability of this system against density fluctuations. In the weak- and the intermediate-coupling regimes with respect to $-U_{\rm BF}$, we show that an effective attractive interaction between bosons mediated by density fluctuations in the Fermi component makes the system unstable below a certain temperature $T_{\rm clp}$ (leading to density collapse). When $U_{\rm BB} = 0$, $T_{\rm clp}$ is always higher than the Bose-Einstein condensation (BEC) temperature $T_{\rm c}$. When $U_{\rm BB} > 0$, the density collapse is suppressed, and the BEC transition becomes possible. It is also suppressed by the formation of tightly bound Bose-Fermi molecules when the heteropairing interaction $-U_{\rm BF}$ is strong; however, since the system may be viewed as a molecular Fermi gas in this case, the BEC transition does not also occur. Since quantum gases involving Bose atoms are known to be sensitive to interparticle correlations, our results would be useful for the study of many-body properties of a Bose-Fermi mixture in a stable manner, without facing the unwanted density collapse.

DOI: 10.1103/PhysRevA.103.063317

I. INTRODUCTION

Recently, Bose-Fermi mixtures have attracted much attention in cold-atom physics [1–7]. Since one can tune the strength of a Bose-Fermi pairing interaction by adjusting the threshold energy of a heteronuclear Feshbach resonance [8], strong-coupling properties of this gas mixture have been studied [9–13]. In addition, tuning of an effective Bose-Bose (Fermi-Fermi) interaction mediated by a Fermi (Bose) component has also been discussed [14–17]. As an interesting possibility, a non-s-wave Fermi superfluid induced by such a boson-mediated pairing interaction has recently been proposed [18–20].

Bose-Fermi mixtures have also been discussed in other research fields, e.g., ^{3}He-^{4}He mixtures [21–23], as well as a high-density QCD matter [24] [where the system is regarded as a mixture of bound diquarks (bosons) and unpaired quarks (fermions)]. In condensed matter physics, as a possible route to reach high-temperature superconductivity, a nanodevice consisting of an n-doped semiconductor (electron gas) immersed in an exciton-polariton Bose-Einstein condensate (bosons) has theoretically been proposed [25–27]. Since a Bose-Fermi mixture in cold-atom physics is simple and highly tunable, this dilute gas system is expected to be a useful quantum simulator [28] for the study of these more complicated many-body quantum systems.

In considering a Bose-Fermi mixture with a heteronuclear Feshbach resonance, besides strong-coupling effects caused by a Feshbach-induced tunable interaction, thermodynamic stability is also a crucial issue [16,29–34]. Indeed, the density collapse of a gas mixture of Bose and Fermi atoms into the trap center has experimentally been reported [29–32]. To simply understand this instability, it would be helpful to recall that a single-component Bose gas with an attractive interaction is unstable [35–39]. In the same manner, a Bose-Fermi mixture may also become unstable by an effective attractive Bose-Bose interaction mediated by Fermi atoms [35,40].

In this paper, we theoretically investigate a Bose-Fermi mixture with a tunable Bose-Fermi pairing interaction associated with a heteronuclear Feshbach resonance. To include strong heteropairing fluctuations caused by the tunable Bose-Fermi attraction, we extend the self-consistent T-matrix approximation (SCTMA) developed for two-component Fermi systems [41–43] to the case where one of the two Fermi components is replaced by bosons. We briefly note that, in cold Fermi gas physics, the SCTMA has been used [44] to study BCS (Bardeen-Cooper-Schrieffer)–BEC (Bose-Einstein condensation) crossover behavior [45–51] of ^{40}K [52] and ^{6}Li [53–55] Fermi gases. In this paper, we employ this strong-coupling theory to evaluate the compressibility matrix of a Bose-Fermi mixture, to unifiedly examine the thermodynamic stability against density fluctuations from the weak- to the strong-coupling regime. In particular, we focus on how an effective Bose-Bose attractive interaction mediated by density fluctuations of fermions makes the system unstable and how this instability is suppressed by strong-coupling effects, as well as a direct Bose-Bose repulsion.

The stability of a Bose-Fermi mixture has been examined by many researchers by various methods: References [56–60]

*kmanabe@rk.phys.keio.ac.jp

discuss this problem within the mean-field approximation. Reference [61] goes beyond the mean-field level to include many-body effects, although the validity is still restricted to the weak-coupling regime. The stability across a Feshbach resonance is examined by a variational method in Ref. [62], which is, however, unable to treat the strong-coupling regime (where tightly bound Bose-Fermi molecules dominate over system properties). Regarding this, we emphasize that the SCTMA has the advantage that it can cover the weak- to the strong-coupling regime. Of course, the SCTMA also still has room for improvement. In this paper, we also assess this approach for future studies.

In this paper, we assume a uniform gas, for simplicity. We briefly note that the effects of a harmonic trap have been examined in Refs. [57–59], where the critical boson number (above which the system becomes unstable) has been discussed by treating the Bose (Fermi) component within the Gross-Pitaevskii equation (Thomas-Fermi approximation).

This paper is organized as follows: In Sec. II, we explain our formulation. In Sec. III, we discuss how an effective Bose-Bose interaction mediated by fermions makes the system unstable at various strengths of a Bose-Fermi pairing interaction. We consider the effects of a direct Bose-Bose repulsion on this instability in Sec. IV, to clarify the condition for the realization of BEC without facing the unwanted density collapse. Throughout this paper, we set $\hbar = k_{\rm B} = 1$, and the system volume V is taken to be unity, for simplicity.

II. FORMULATION

We consider a gas mixture of single-component Bose atoms and single-component Fermi atoms, described by the Hamiltonian

$$H = \sum_{\boldsymbol{p}} \left[\xi_p^{\rm F} f_{\boldsymbol{p}}^\dagger f_{\boldsymbol{p}} + \xi_p^{\rm B} b_{\boldsymbol{p}}^\dagger b_{\boldsymbol{p}}\right] - U_{\rm BF} \times \sum_{\boldsymbol{p},\boldsymbol{p}',\boldsymbol{q}} f_{\boldsymbol{p}+\frac{\boldsymbol{q}}{2}}^\dagger b_{-\boldsymbol{p}+\frac{\boldsymbol{q}}{2}}^\dagger b_{-\boldsymbol{p}'+\frac{\boldsymbol{q}}{2}} f_{\boldsymbol{p}'+\frac{\boldsymbol{q}}{2}} + \frac{U_{\rm BB}}{2} \sum_{\boldsymbol{p},\boldsymbol{p}',\boldsymbol{q}} b_{\boldsymbol{p}+\frac{\boldsymbol{q}}{2}}^\dagger b_{-\boldsymbol{p}+\frac{\boldsymbol{q}}{2}}^\dagger b_{-\boldsymbol{p}'+\frac{\boldsymbol{q}}{2}} b_{\boldsymbol{p}'+\frac{\boldsymbol{q}}{2}}. \tag{1}$$

Here, $b_{\boldsymbol{p}}^\dagger$ ($f_{\boldsymbol{p}}^\dagger$) is the creation operator of a Bose (Fermi) atom with momentum $\boldsymbol{p}$. $\xi_p^{\alpha={\rm B,F}} = \boldsymbol{p}^2/(2m_\alpha) - \mu_\alpha$ is the kinetic energy of the α component, measured from the chemical potential μ_α (where m_α is an atomic mass). In this paper, we only deal with the mass-balanced ($m_{\rm F} = m_{\rm B} \equiv m$) and population-balanced ($N_{\rm B} = N_{\rm F} \equiv N$) case, for simplicity (where $N_{\rm B}$ and $N_{\rm F}$ are the numbers of Bose and Fermi atoms, respectively). $-U_{\rm BF}(<0)$ is an attractive interaction between Bose and Fermi atoms, which is assumed to be tunable by adjusting the threshold energy of a heteronuclear Feshbach resonance. As usual, we measure the strength of this tunable interaction in terms of the Bose-Fermi s-wave scattering length $a_{\rm BF}$, given by

$$\frac{4\pi a_{\rm BF}}{m} = -\frac{U_{\rm BF}}{1 - U_{\rm BF}\sum_{\boldsymbol{p}}^{p_{\rm c}} \frac{m}{p^2}}, \tag{2}$$

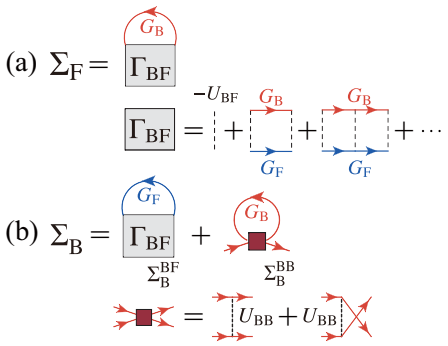

FIG. 1. Self-energy corrections considered in this paper. (a) Fermi component $\Sigma_{\rm F}$. The particle-particle scattering matrix $\Gamma_{\rm BF}$ describes heteropairing fluctuations associated with the Bose-Fermi attractive interaction $-U_{\rm BF}(<0)$ (dashed lines). $G_{\rm F}$ and $G_{\rm B}$ represent the dressed single-particle Fermi and Bose Green's functions, respectively. (b) Bose component $\Sigma_{\rm B} = \Sigma_{\rm B}^{\rm BF} + \Sigma_{\rm B}^{\rm BB}$, consisting of the contribution from heteropairing fluctuations ($\Sigma_{\rm B}^{\rm BF}$) and that from a weak Bose-Bose repulsion $U_{\rm BB}(\gtrsim 0)$ ($\Sigma_{\rm B}^{\rm BB}$). For later convenience, the symmetrized interaction (red squares) is introduced for $U_{\rm BB}$. In this paper, we treat $-U_{\rm BF}$ in SCTMA and $U_{\rm BB}$ in the mean-field level.

where $p_{\rm c}$ is the high-momentum cutoff. In Eq. (1), $U_{\rm BB}(\gtrsim 0)$ is a (direct) repulsive interaction between Bose atoms, which has nothing to do with an "effective" Bose-Bose interaction *mediated by Fermi atoms* (which appears in later discussion). We assume that it is weak and constant across a heteronuclear Feshbach resonance. For later convenience, we introduce another s-wave scattering length, $a_{\rm BB}$, for $U_{\rm BB}$, given by, in the Born approximation [35],

$$\frac{4\pi a_{\rm BB}}{m} = U_{\rm BB}. \tag{3}$$

Of course, the s-wave interaction does not work between Fermi atoms due to Pauli's exclusion principle.

Effects of $-U_{\rm BF}$ and $U_{\rm BB}$ on single-particle properties of the system can conveniently be incorporated into the self-energies $\Sigma_{\alpha={\rm B,F}}(p)$ in the Bose ($\alpha = {\rm B}$) and Fermi ($\alpha = {\rm F}$) single-particle thermal Green's functions,

$$G_{\alpha={\rm B,F}}(p) = \frac{1}{i\omega_n^\alpha - \xi_{\boldsymbol{p}}^\alpha - \Sigma_\alpha(p)}. \tag{4}$$

Here, we have introduced the abbreviated notation $p = (\boldsymbol{p}, i\omega_n^\alpha)$, where $\omega_n^{\rm B}$ and $\omega_n^{\rm F}$ are the boson and fermion Matsubara frequencies, respectively [63].

To include strong heteropairing fluctuations associated with $-U_{\rm BF}$, we extend the SCTMA developed in the BCS-BEC crossover physics of Fermi superfluids [41–44] to the present case. An advantage of the SCTMA is that it is a Φ-derivable approximation [43,64–66], which allows us to calculate thermodynamic quantities in a consistent manner. The SCTMA fermion self-energy $\Sigma_{\rm F}$ associated with the heteropairing interaction $-U_{\rm BF}$ is diagrammatically drawn in Fig. 1(a), which gives

$$\Sigma_{\rm F}(p) = -T\sum_q \Gamma_{\rm BF}(q) G_{\rm B}(q-p). \tag{5}$$

Here, the particle-particle scattering matrix,

$$\Gamma_{\rm BF}(q) = \frac{-U_{\rm BF}}{1 - U_{\rm BF}\Pi_{\rm BF}(q)} = \frac{1}{\frac{m}{4\pi a_{\rm BF}} + \left[\Pi_{\rm BF}(q) - \sum_{\boldsymbol{p}}^{p_{\rm c}} \frac{m}{p^2}\right]}, \tag{6}$$

physically describes heteropairing fluctuations. In Eq. (6),

$$\Pi_{\rm BF}(q) = T\sum_k G_{\rm F}(q-k)G_{\rm B}(k) \tag{7}$$

is the Bose-Fermi pair-correlation function. The SCTMA boson self-energy $\Sigma_{\rm B} = \Sigma_{\rm B}^{\rm BF} + \Sigma_{\rm B}^{\rm BB}$ in Fig. 1(b) involves the effects of (i) Bose-Fermi attraction $-U_{\rm BF}$ ($=\Sigma_{\rm B}^{\rm BF}$) and (ii) direct Bose-Bose repulsion $U_{\rm BB}$ ($=\Sigma_{\rm B}^{\rm BB}$). The former is given by

$$\Sigma_{\rm B}^{\rm BF}(p) = T\sum_q \Gamma_{\rm BF}(q)G_{\rm F}(q-p). \tag{8}$$

For $\Sigma_{\rm B}^{\rm BB}$, assuming that $U_{\rm BB}$ is weak, we simply treat it within the mean-field approximation, which gives

$$\Sigma_{\rm B}^{\rm BB} = \frac{8\pi a_{\rm BB}}{m}N. \tag{9}$$

We briefly note that the (non-self-consistent) T-matrix approximation (TMA) [10,11,67] is immediately obtained by replacing all the dressed Green's functions G_α in Fig. 1 with the bare ones,

$$G_\alpha^0(p) = \frac{1}{i\omega_n^\alpha - \xi_{\boldsymbol{p}}^\alpha}. \tag{10}$$

As shown later, the TMA is not suitable for our purpose, because it cannot capture the collapse of a Bose-Fermi mixture.

We determine the BEC phase transition temperature $T_{\rm c}$ from the Hugenholtz-Pines theorem [68], which states that the Bose excitations become gapless at $T_{\rm c}$:

$$\mu_{\rm B} - \Sigma_{\rm B}(p=0) = 0. \tag{11}$$

We solve Eq. (11), together with the number equations,

$$N_{\rm B} = -T\sum_p G_{\rm B}(p), \tag{12}$$

$$N_{\rm F} = T\sum_p G_{\rm F}(p), \tag{13}$$

to self-consistently determine $T_{\rm c}$ and $\mu_\alpha(T_{\rm c})$ for given interaction strengths. Above $T_{\rm c}$, we only deal with the number equations, (12) and (13), to determine $\mu_\alpha(T > T_{\rm c})$.

Figure 2 shows the SCTMA solutions of $\mu_{\rm F}(T \geqslant T_{\rm c})$ and $\mu_{\rm B}(T \geqslant T_{\rm c})$, when $U_{\rm BB} = 0$. As previously obtained within a modified TMA scheme [12], $T_{\rm c}$ vanishes at $(k_{\rm F}a_{\rm BF})^{-1} \simeq 0.9$ [QCP (quantum critical point) in this figure], and the BEC phase transition no longer occurs for stronger Bose-Fermi interactions. We briefly note that, because we treat $U_{\rm BB}$ within the mean-field approximation [see Eq. (9)], $\mu_{\alpha={\rm F,B}}$ with $U_{\rm BB} > 0$ are immediately obtained from the results in

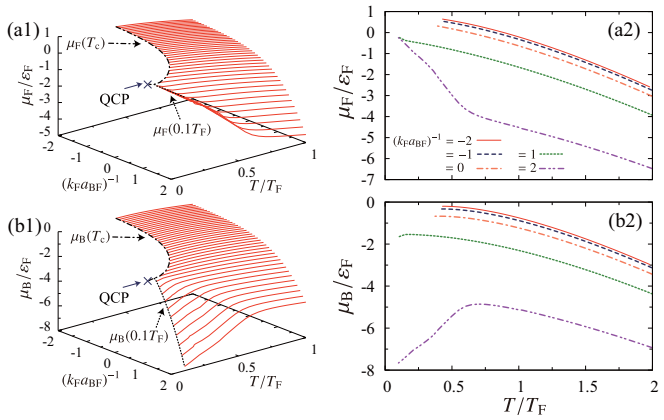

FIG. 2. Calculated chemical potentials μ_α in the SCTMA in the normal state of a Bose-Fermi mixture, above the BEC phase transition temperature $T_{\rm c}$. We set $U_{\rm BB} = 0$. (a1, a2) $\mu_{\rm F}(T)$. (b1, b2) $\mu_{\rm B}(T)$. The strength of a Bose-Fermi interaction is measured in terms of the inverse scattering length $a_{\rm BF}^{-1}$ in Eq. (2), normalized by the Fermi momentum $k_{\rm F} = (6\pi^2 N)^{1/3}$. $\varepsilon_{\rm F} = k_{\rm F}^2/(2m)$ and $T_{\rm F}$ ($=\varepsilon_{\rm F}$) are the Fermi energy and the Fermi temperature, respectively. QCP denotes the quantum critical point at which $T_{\rm c}$ vanishes. Due to numerical difficulty, calculations in the strong-coupling region are restricted to $T \geqslant 0.1T_{\rm F}$. We briefly note that the inclusion of nonzero $U_{\rm BB}$ only causes a constant shift of $\mu_{\rm B}$ within the present mean-field approximation.

Fig. 2 as

$$\begin{cases} \mu_{\rm F}(U_{\rm BB} > 0) = \mu_{\rm F}(U_{\rm BB} = 0), \\ \mu_{\rm B}(U_{\rm BB} > 0) = \mu_{\rm B}(U_{\rm BB} = 0) + \Sigma_{\rm B}^{\rm BB}. \end{cases} \tag{14}$$

Using the SCTMA solutions, we evaluate the compressibility matrix $\hat{\kappa} = \{\kappa_{\alpha\beta}\}$ ($\alpha, \beta = {\rm F, B}$) [69] to assess the stability of a Bose-Fermi mixture against density fluctuations. The matrix elements $\kappa_{\alpha\beta}$ are given by

$$\kappa_{\alpha\beta} = \frac{\partial N_\alpha}{\partial \mu_\beta}. \tag{15}$$

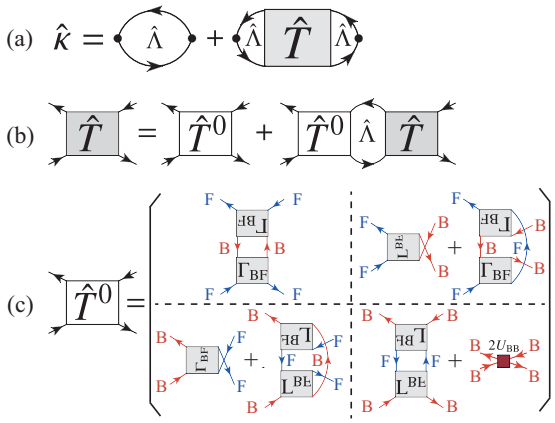

FIG. 3. (a) Diagrammatic representation of compressibility matrix $\hat{\kappa}$. $\hat{\Lambda}$ is given in Eq. (18). $\hat{T}(p, p')$ is the 2×2 matrix four-point vertex, which obeys the Bethe-Salpeter equation in (b). (c) Irreducible four-point vertex $\hat{T}^0$ appearing in (b). The particle-particle scattering matrix $\Gamma_{\rm BF}$ is given in Fig. 1(a). Solid lines labeled "F" ("B") are the dressed Fermi (Bose) Green's functions in Eq. (4).

In this paper, we numerically evaluate Eq. (15). The system is stable if and only if $\hat{\kappa}$ is *positive definite*, that is, the following conditions are satisfied:

$$\begin{cases} \kappa_{\rm BB} > 0 \quad (\text{or} \quad \kappa_{\rm FF} > 0), \\ \det[\hat{\kappa}] > 0. \end{cases} \tag{16}$$

For the derivation of this stability condition, see Appendix A.

We evaluate interaction corrections to the compressibility matrix $\hat{\kappa}$, so as to be consistent with the self-energy corrections $\Sigma_{\alpha={\rm F,B}}$ in Fig. 1. This condition is immediately satisfied, when we substitute the number equations, (12) and (13), into Eq. (15). The result is

$$\hat{\kappa} = \begin{pmatrix} \kappa_{\rm FF} & \kappa_{\rm FB} \\ \kappa_{\rm BF} & \kappa_{\rm BB} \end{pmatrix} = T\sum_{p} \hat{\Lambda}(p) - T^2 \sum_{p,p'} \hat{\Lambda}(p)\hat{T}(p,p')\hat{\Lambda}(p'), \tag{17}$$

which is diagrammatically described as Fig. 3(a). Here,

$$\hat{\Lambda}(p) = \begin{pmatrix} -G_{\rm F}^2(p) & 0 \\ 0 & G_{\rm B}^2(p) \end{pmatrix}, \tag{18}$$

and the 2×2 matrix four-point vertex $\hat{T}(p,p')$ obeys the Bethe-Salpeter equation [70], which is shown diagrammatically in Fig. 3(b). The expression of this equation is given by

$$\hat{T}(p,p') = \hat{T}^0(p,p') - T\sum_{q} \hat{T}^0(p,q)\hat{\Lambda}(q)\hat{T}(q,p'), \tag{19}$$

where the irreducible part $\hat{T}^0$ has the form [see also Fig. 3(c)]

$$\hat{T}_0(p,p') = \begin{pmatrix} 0 & 0 \\ 0 & \frac{8\pi a_{\rm BB}}{m} \end{pmatrix} + \begin{pmatrix} 0 & \Gamma_{\rm BF}(p+p') \\ \Gamma_{\rm BF}(p+p') & 0 \end{pmatrix} - T\sum_{q} \Gamma_{\rm BF}^2(q) \begin{pmatrix} -G_{\rm B}(q-p)G_{\rm B}(q-p') & G_{\rm B}(q-p)G_{\rm F}(q-p') \\ G_{\rm F}(q-p)G_{\rm B}(q-p') & -G_{\rm F}(q-p)G_{\rm F}(q-p') \end{pmatrix}. \tag{20}$$

We briefly note that the second and third terms in Eq. (20) give, respectively, Maki-Thompson (MT)–type [71–73] and Aslamazov-Larkin (AL)–type [73,74] fluctuation corrections to $\hat{\kappa}$.

In the noninteracting case ($U_{\rm BF} = U_{\rm BB} = 0$), the first term in Eq. (17) is reduced to the compressibility matrix in a mixture of ideal Fermi gas and ideal Bose gas, given by

$$\hat{\kappa}_0 \equiv \begin{pmatrix} \kappa_{\rm FF}^0 & 0 \\ 0 & \kappa_{\rm BB}^0 \end{pmatrix} = \sum_{p} \begin{pmatrix} \Lambda_{\rm FF}^0(\xi_p^{\rm F}) & 0 \\ 0 & \Lambda_{\rm BB}^0(\xi_p^{\rm B}) \end{pmatrix}. \tag{21}$$

Here,

$$\Lambda_{\alpha\alpha}^0(\xi_p^\alpha) = \frac{\partial f_\alpha(\xi_p^\alpha)}{\partial \mu_\alpha}, \tag{22}$$

where $f_{\rm F}(\xi_p^{\rm F})$ and $f_{\rm B}(\xi_p^{\rm B})$ are the Fermi and Bose distribution functions, respectively. As expected, Eq. (21) satisfies both the stability conditions in Eq. (16).

III. STABILITY OF A BOSE-FERMI MIXTURE WHEN $U_{\rm BB} = 0$

A. Weak-coupling side: Simultaneous density collapse of Bose and Fermi components

In this section, we set $U_{\rm BB} = 0$. Figures 4(a)–4(c) show the compressibilities $\kappa_{\alpha\beta}$ ($\alpha, \beta = {\rm F, B}$) in this case, as functions of the temperature and the strength $(k_{\rm F}a_{\rm BF})^{-1}$ of the Bose-Fermi pairing interaction. All the compressibility components $\kappa_{\alpha\beta}$ are found to monotonically increase with decreasing temperature, to diverge at the same collapse temperature $T_{\rm clp}$. For clarity, the interaction dependence of $T_{\rm clp}$ is separately shown in Fig. 4(d). This simultaneous instability of the Bose and Fermi components is consistent with the density collapse observed in ^{87}Rb - ^{40}K mixtures [29–32].

To clearly show this singular behavior of $\kappa_{\alpha\beta}$ at $T_{\rm clp}$, as an example, we extract the results at unitarity in Fig. 5(a): One of the stability conditions $\kappa_{\rm BB} > 0$ in Eq. (16) is found not to be satisfied below $T_{\rm clp}$, indicating the occurrence of density

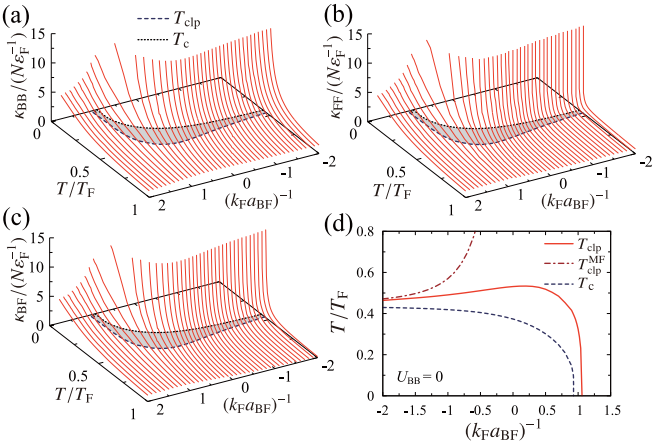

FIG. 4. (a)–(c) Calculated compressibilities $\kappa_{\alpha\beta}$ in a Bose-Fermi mixture, when $U_{\rm BB} = 0$. (a) $\kappa_{\rm BB}$. (b) $\kappa_{\rm FF}$. (c) $\kappa_{\rm BF}$ ($= \kappa_{\rm FB}$). All these compressibilities diverge at the same collapse temperature $T_{\rm clp}$, shown as the dashed line in the temperature-interaction plane. In the shaded region between $T_{\rm clp}$ and the BEC phase transition temperature $T_{\rm c}$ (dotted line), the compressibilities are negative, although we do not explicitly show $\kappa_{\alpha\beta}$ there. For clarity, we show $T_{\rm clp}$ and $T_{\rm c}$ as functions of the Bose-Fermi interaction strength $[(k_{\rm F}a_{\rm BF})^{-1}]$ in (d). $T_{\rm clp}^{\rm MF}$ is obtained from the condition that the denominator of Eq. (27) vanishes.

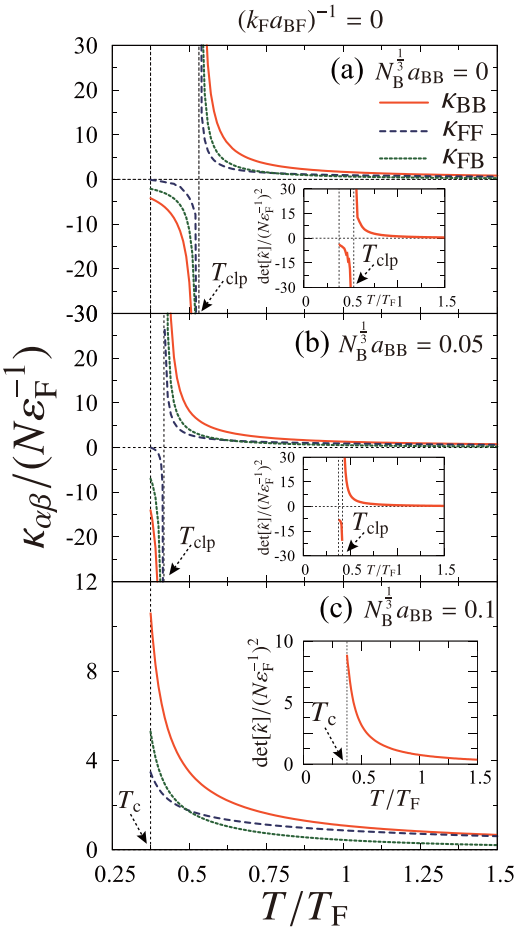

FIG. 5. Compressibilities $\kappa_{\alpha\beta}$ in the unitary limit $[(k_F a_{BF})^{-1}=0]$. (a) $N_B^{1/3} a_{BB} = 0$ ($U_{BB} = 0$). (b) $N_B^{1/3} a_{BB} = 0.05$. (c) $N_B^{1/3} a_{BB} = 0.1$. Insets: $\det[\hat{\kappa}]$. We note that T_c is unaffected by U_{BB} within the present mean-field approximation.

collapse [35,56–62]. Above T_{clp}, the stability conditions in Eq. (16) are all satisfied, so that the system is thermodynamically stable there. The same results are also obtained when $(k_F a_{BF})^{-1} \neq 0$, although we do not explicitly show the results here. We also find from Fig. 4(d) that, with decreasing temperature, the system always collapses before reaching the BEC phase transition, at least when $U_{BB} = 0$.

To grasp the background physics of this phenomenon at T_{clp}, it is convenient to consider the weak-coupling regime $[(k_F a_{BF})^{-1} \lesssim -1]$. In this regime, since heteropairing fluctuations are weak, one may safely approximate the Bose-Fermi scattering matrix $\Gamma_{BF}(q)$ to the constant weak attractive interaction,

$$\tilde{\Gamma}_{BF} \equiv \frac{4\pi a_{BF}}{m} \quad (a_{BF} < 0). \tag{23}$$

The self-energies in Eqs. (5) and (8) are then reduced to the mean-field ones,

$$\Sigma_\alpha^{MF} = \tilde{\Gamma}_{BF} N_{-\alpha}, \tag{24}$$

where $-\alpha$ means the opposite component to $\alpha = F, B$. (Note that we are setting $U_{BB} = 0$ here, so that $\Sigma_B = \Sigma_B^{BF} + \Sigma_B^{BB} = \Sigma_B^{BF}$.)

Using Eqs. (4), (13), (15), and (24), we obtain the Bose compressibility κ_{BB} as

$$\kappa_{BB} = \frac{\partial N_B}{\partial \mu_B} = T \sum_p G_B^2(p) \left[1 - \frac{\partial \Sigma_B^{MF}}{\partial \mu_B} \right]$$
$$= \tilde{\kappa}_{BB}^0 \left[1 - \tilde{\Gamma}_{BF} \kappa_{FB} \right]. \tag{25}$$

Here, $\tilde{\kappa}_{BB}^0$ is given by κ_{BB}^0 in Eq. (21) with the kinetic energy ξ_p^B replaced by $\tilde{\xi}_p^B \equiv \xi_p^B + \Sigma_{BB}^{MF}$. The off-diagonal compressibility $\kappa_{FB} = \partial N_F / \partial \mu_B$ in Eq. (25) is calculated in the same manner,

$$\kappa_{FB} = -\tilde{\kappa}_{FF}^0 \tilde{\Gamma}_{BF} \kappa_{BB}, \tag{26}$$

where $\tilde{\kappa}_{FF}^0$ is obtained from κ_{FF}^0 in Eq. (21) by replacing ξ_p^F with $\tilde{\xi}_p^F \equiv \xi_p^F + \Sigma_{FF}^{MF}$. Substituting Eq. (26) into Eq. (25), we reach

$$\kappa_{BB} = \frac{\tilde{\kappa}_{BB}^0}{1 - \tilde{\Gamma}_{BF}^2 \tilde{\kappa}_{FF}^0 \tilde{\kappa}_{BB}^0}. \tag{27}$$

The Fermi compressibility κ_{FF} can also be evaluated in the same manner, giving

$$\kappa_{FF} = \tilde{\kappa}_{FF}^0 + \left(\tilde{\Gamma}_{BF} \tilde{\kappa}_{FF}^0 \right) \kappa_{BB} \left(\tilde{\Gamma}_{BF} \tilde{\kappa}_{FF}^0 \right). \tag{28}$$

In the weak-coupling regime, $\tilde{\kappa}_{FF}^0$ approaches a constant value [$\simeq \rho_F(0) > 0$, where $\rho_F(0)$ is the Fermi single-particle density of states at the Fermi level] far below the Fermi temperature T_F. On the other hand, because $\tilde{\kappa}_{BB}^0$ has the same form as the compressibility in an ideal Bose gas, it diverges at the BEC phase transition temperature T_c. Thus, κ_{BB} in Eq. (27) always diverges at the temperature ($\equiv T_{clp}^{MF} > T_c$) at which the denominator of this equation vanishes. We see in Eq. (28) that this singularity is immediately brought to the Fermi compressibility through the "Bose-Fermi coupling" $\tilde{\Gamma}_{BF}$, leading to the simultaneous density collapse.

We note that Eq. (27) has the same form as the compressibility in a Bose gas with the *attractive* interaction,

$$V_{BB}^{eff} \equiv -\tilde{\Gamma}_{BF}^2 \tilde{\kappa}_{FF}^0, \tag{29}$$

in the random phase approximation (RPA). Recalling that a Bose gas is unstable against an attractive interaction [35], the present simultaneous collapse phenomenon is found also to come from this attractive interaction V_{BB}^{eff}. The fact that Eq. (29) involves the Fermi compressibility $\tilde{\kappa}_{FF}^0$ means that it is medicated by density fluctuations in the Fermi component.

We compare T_{clp}^{MF} with T_{clp} in Fig. 4(d). Although the above discussion is based on the simple approximation in Eq. (23), the calculated T_{clp}^{MF} agrees well with the SCTMA result in the weak-coupling regime $[(k_F a_{BF})^{-1} \lesssim -1]$.

We emphasize that, in obtaining the above results about the simultaneous density collapse, the fact that the SCTMA uses the dressed Green's functions $G_{\alpha=F,B}$ is crucial. Indeed, as shown in Fig. 6, this phenomenon cannot be explained in the TMA, where all the dressed Green's functions in Fig. 1 are replaced by the *bare* ones G_α^0 [10,11,67]: The Fermi compressibility κ_{FF}^{TMA} in the TMA does *not* diverge down to the BEC phase transition temperature. In addition, the required symmetry property,

$$\kappa_{BF} = \frac{\partial N_B}{\partial \mu_F} = -\frac{\partial^2 \Omega}{\partial \mu_F \partial \mu_B} = \frac{\partial N_F}{\partial \mu_B} = \kappa_{FB}, \tag{30}$$

is broken in TMA, as shown in Fig. 6.

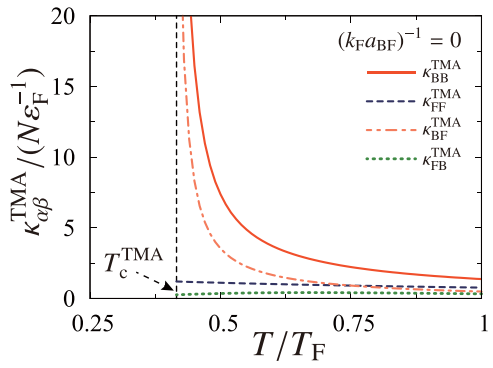

FIG. 6. Calculated TMA compressibilities $\kappa^{\rm TMA}_{\alpha\beta}$ in the unitary limit. $T_{\rm c}^{\rm TMA}$ is the BEC transition temperature in the TMA.

To explain the reason for these TMA results, we again approximate $\Gamma_{\rm BF}(q)$ to $\tilde{\Gamma}_{\rm BF}$ in Eq. (23). We then find that the key is that the particle number $N_{-\alpha}$ in Eq. (24) [which equals $\sum_{\boldsymbol{p}} f_{-\alpha}(\xi_{\boldsymbol{p}}^{-\alpha} + \Sigma_{-\alpha}^{\rm MF})$ in the SCTMA] is replaced by $N_{-\alpha}^0 = \sum_{\boldsymbol{p}} f_{-\alpha}(\xi_{\boldsymbol{p}}^{-\alpha})$ in the TMA, because the bare Green's functions are used in the latter theory. Noting that $\partial N_\alpha^0/\partial\mu_{-\alpha} = 0$, we immediately obtain $\kappa_{\rm BB} = \tilde{\kappa}^0_{\rm BB}$ and $\kappa_{\rm FF} = \tilde{\kappa}^0_{\rm FF}$. That is, although the Bose compressibility $\kappa_{\rm BB}$ still diverges at the BEC phase transition (because $\tilde{\kappa}^0_{\rm BB} \to \infty$), it does not affect the Fermi compressibility $\kappa_{\rm FF}$ in the TMA case. In addition, when $N^0_{-\alpha}$ is used for $N_{-\alpha}$ in Eq. (24), we also obtain the breakdown of the symmetry property $\kappa_{\rm BF} \neq \kappa_{\rm FB}$ as

$$\kappa_{\rm BF} = \tilde{\kappa}^0_{\rm BB}\tilde{\Gamma}_{\rm BF}\kappa^0_{\rm FF}, \tag{31}$$

$$\kappa_{\rm FB} = \kappa^0_{\rm BB}\tilde{\Gamma}_{\rm BF}\tilde{\kappa}^0_{\rm FF} \neq \kappa_{\rm BF}. \tag{32}$$

However, the present SCTMA approach also has room for improvement, e.g., with respect to Pauli's exclusion principle: To explain this, we again use the approximation in Eq. (23) to rewrite the last term in Eq. (28) ($\equiv\Delta\kappa_{\rm FF}$) into the form of the first-order perturbation in terms of the effective Fermi-Fermi interaction,

$$H_{\rm eff} = \frac{1}{2}\sum_{\boldsymbol{p},\boldsymbol{p}',\boldsymbol{q}} V^{\rm eff}_{\rm FF}(\boldsymbol{q}) f^\dagger_{\boldsymbol{p}+\boldsymbol{q}} f^\dagger_{\boldsymbol{p}'-\boldsymbol{q}} f_{\boldsymbol{p}'} f_{\boldsymbol{p}}, \tag{33}$$

as

$$\Delta\kappa_{\rm FF} = -\sum_{\boldsymbol{p},\boldsymbol{p}'} \Lambda^0_{\rm FF}\big(\tilde{\xi}^{\rm F}_{\boldsymbol{p}}\big) V^{\rm eff}_{\rm FF}(0) \Lambda^0_{\rm FF}\big(\tilde{\xi}^{\rm F}_{\boldsymbol{p}'}\big). \tag{34}$$

Here, $\Lambda^0_{\rm FF}$ is given in Eq. (22), and

$$V^{\rm eff}_{\rm FF}(\boldsymbol{q}) = \frac{-\tilde{\Gamma}^2_{\rm BF}\tilde{\kappa}^0_{\rm BB}(\boldsymbol{q})}{1 - \tilde{\Gamma}^2_{\rm BF}\tilde{\kappa}^0_{\rm FF}(\boldsymbol{q})\tilde{\kappa}^0_{\rm BB}(\boldsymbol{q})}, \tag{35}$$

where

$$\tilde{\kappa}_{\alpha\alpha}(\boldsymbol{q}) = \sum_{\boldsymbol{k}} \frac{f_\alpha\big(\tilde{\xi}^\alpha_{\boldsymbol{k}+\boldsymbol{q}}\big) - f_\alpha\big(\tilde{\xi}^\alpha_{\boldsymbol{k}}\big)}{\tilde{\xi}^\alpha_{\boldsymbol{k}+\boldsymbol{q}} - \tilde{\xi}^\alpha_{\boldsymbol{k}}}. \tag{36}$$

Noting that Eq. (34) is diagrammatically described as Fig. 7(a), it involves the unphysical case with $\boldsymbol{p}' = \boldsymbol{p}$, which corresponds to the scattering of two Fermi atoms in the *same* quantum state. This serious problem is removed by taking into account the other correction to $\kappa_{\rm FF}$ given in Fig. 7(b). This modifies Eq. (34) as

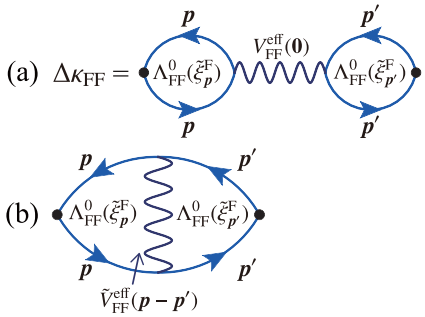

FIG. 7. (a) Diagrammatic representation of the last term in Eq. (28) ($=\Delta\kappa_{\rm FF}$) using the effective Fermi-Fermi interaction $V^{\rm eff}_{\rm FF}(\boldsymbol{q})$ (wavy line) in Eq. (35). The solid line is the Fermi single-particle Green's function $G_{\rm F}$ with the self-energy $\Sigma^{\rm MF}_{\rm F}$ in Eq. (24). (b) Another correction to $\kappa_{\rm FF}$. It recovers Pauli's exclusion principle when $\tilde{V}^{\rm eff}_{\rm FF}(\boldsymbol{p}-\boldsymbol{p}') = V^{\rm eff}_{\rm FF}(\boldsymbol{p}-\boldsymbol{p}')$.

$$\Delta\kappa_{\rm FF} = -\sum_{\boldsymbol{p},\boldsymbol{p}'} \Lambda^0_{\rm FF}\big(\tilde{\xi}^{\rm F}_{\boldsymbol{p}}\big)\big[V^{\rm eff}_{\rm FF}(0) - \tilde{V}^{\rm eff}_{\rm FF}(\boldsymbol{p}-\boldsymbol{p}')\big]\Lambda^0_{\rm FF}\big(\tilde{\xi}^{\rm F}_{\boldsymbol{p}'}\big). \tag{37}$$

The unwanted contribution at $\boldsymbol{p}' = \boldsymbol{p}$ (which contradicts Pauli's exclusion principle) is now canceled out by the additional term when $\tilde{V}^{\rm eff}_{\rm FF}(\boldsymbol{p}-\boldsymbol{p}') = V^{\rm eff}_{\rm FF}(\boldsymbol{p}-\boldsymbol{p}')$.

Regarding this problem, the SCTMA Fermi compressibility $\kappa_{\rm FF}$ involves the contribution being similar to Fig. 7(b), which is obtained from the (11)-component of the irreducible four-point vertex $\hat{T}^0$ shown in Fig. 3(c). However, it is still insufficient to fully recover Pauli's exclusion principle. [This situation corresponds to $\tilde{V}^{\rm eff}_{\rm FF}(\boldsymbol{p}-\boldsymbol{p}') \neq V^{\rm eff}_{\rm FF}(\boldsymbol{p}-\boldsymbol{p}')$ in the above approximate discussion.] Because the simultaneous density collapse is caused by the divergence of $V^{\rm eff}_{\rm FF}(0) \propto \kappa_{\rm BB}$, this incomplete cancellation at $\boldsymbol{p}' = \boldsymbol{p}$ means that the diverging contribution to $\kappa_{\rm F}(T = T_{\rm clp})$ around $\boldsymbol{p}' = \boldsymbol{p}$ is overestimated to some extent in the SCTMA. Thus, to *quantitatively* discuss the density collapse in a Bose-Fermi mixture, we need to improve the SCTMA, which remains our future problem. We briefly note that a similar problem has also been discussed in condensed matter physics (see Ref. [75]).

B. Strong-coupling side: Composite Fermi-molecular gas

We see in Fig. 4(d) that the collapse temperature $T_{\rm clp}$ increases with increasing Bose-Fermi interaction strength on the weak-coupling side $(k_F a_{\rm BF})^{-1} \lesssim 0$. Because the mean-field result $T^{\rm MF}_{\rm clp}$ also exhibits the same tendency in this regime, this behavior is considered to originate from the increase in the strength of the fermion-mediated Bose-Bose attractive interaction, as a result of the enhancement of heteropairing fluctuations described by $\Gamma_{\rm BF}(q)$ [see $V^{\rm eff}_{\rm BB}$ in Eq. (29)].

However, $T_{\rm clp}$ gradually deviates from $T^{\rm MF}_{\rm clp}$, as one passes through the unitary limit, to eventually vanish at $(k_F a_{\rm BF})^{-1} \simeq 1.1$, as shown in Fig. 4(d). This is due to the weakening of the bosonic character of the system, as a result of the formation of two-body composite molecular fermions on the strong-coupling side [$(k_F a_{\rm BF})^{-1} \gtrsim 0$]. Indeed, estimating the number $N_{\rm CF}$ of (quasi-)stable molecular fermions using the method

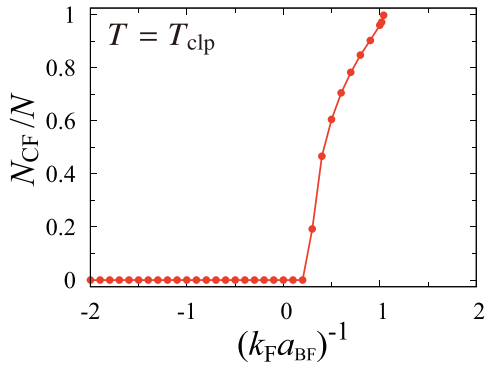

FIG. 8. The number $N_{\rm CF}$ of (quasi-)stable Fermi molecules at $T_{\rm clp}$.

discussed in Ref. [76], we find in Fig. 8 that $T_{\rm clp}$ vanishes when the system becomes dominated by Fermi molecules ($N_{\rm CF} \simeq N$). (We outline how to estimate $N_{\rm CF}$ in Appendix B.) For the same reason, $T_{\rm c}$ also vanishes around the same interaction strength [see Fig. 4(d)]. Thus, when $(k_{\rm F}a_{\rm BF})^{-1} \gtrsim 1.1$, the system may be viewed as a molecular Fermi gas, rather than an atomic Bose-Fermi mixture.

Figure 9 shows the compressibilities $\kappa_{\alpha\beta}$ when $(k_{\rm F}a_{\rm BF})^{-1} = 2 > 1.1$ (where $T_{\rm clp}$ vanishes). In this strong-coupling case, we see in inset (a) that all the compressibility components are almost the same; however, as shown in inset (b), $\det[\hat{\kappa}]$ is still positive, at least within our numerical accuracy. Together with $\kappa_{\alpha\alpha} > 0$, the system in this regime is concluded to be stable against density fluctuations. To examine how the tightly bound Bose-Fermi molecules contribute to the compressibility in Fig. 9, we recall that, deep inside the strong-coupling regime [$(k_{\rm F}a_{\rm BF})^{-1} \gg 1$], the particle-particle scattering matrix $\Gamma_{\rm BF}(q)$ in Eq. (6) is reduced to the molecular Green's function as [11,41] [see also Fig. 10(a)]

$$\Gamma_{\rm BF}(q) \simeq Z_{\rm CF}\mathcal{G}_{\rm CF}(q), \tag{38}$$

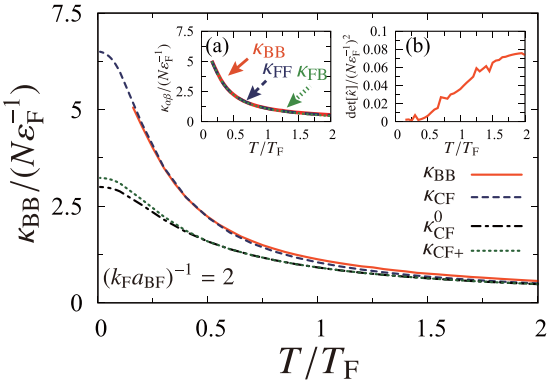

FIG. 9. Calculated SCTMA Bose compressibility $\kappa_{\rm BB}$ as a function of the temperature, when $(k_{\rm F}a_{\rm BF})^{-1} = 2$ (strong-coupling regime). $\kappa_{\rm CF}$ and $\kappa^0_{\rm CF}$ are given in Eqs. (43) and (44), respectively. $\kappa_{\rm CF+}$ shows the result in the case where the last term in Fig. 10(b) is added to $V^{\rm eff}_{\rm CF}$. Inset (a): $\kappa_{\rm FF}$ and $\kappa_{\rm FB}(=\kappa_{\rm BF})$ as functions of the temperature. Inset (b): $\det[\hat{\kappa}]$.

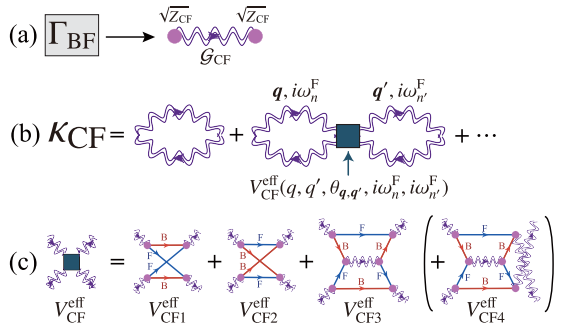

FIG. 10. (a) Relation between the SCTMA particle-particle scattering matrix $\Gamma_{\rm BF}(q)$ and the molecular Green's function $\mathcal{G}_{\rm CF}$ in Eq. (39), deep inside the strong-coupling regime. The renormalization factor $Z_{\rm CF}$ is given below Eq. (38). (b) Diagrammatic representation of $\kappa_{\rm CF}$ appearing in Eq. (41). The double wavy line denotes $\mathcal{G}_{\rm CF}(q)$ in (a). (c) Effective intermolecular interaction $V^{\rm eff}_{\rm CF}$ (filled square) mediated by unpaired atoms. While the first three terms, $V^{\rm eff}_{\rm CF1}$, $V^{\rm eff}_{\rm CF2}$, and $V^{\rm eff}_{\rm CF3}$, are involved in the SCTMA, the last one, $V^{\rm eff}_{\rm CF4}$, is not.

where $Z_{\rm CF} = 8\pi/(m^2 a_{\rm BF})$ and

$$\mathcal{G}_{\rm CF}(q) = \frac{1}{i\omega_n^{\rm F} - \xi_{\boldsymbol{q}}^{\rm CF}}. \tag{39}$$

In Eq. (39), $\xi_{\boldsymbol{q}}^{\rm CF} = \boldsymbol{q}^2/(4m) - \mu_{\rm CF}$ is the molecular kinetic energy, measured from the molecular chemical potential,

$$\mu_{\rm CF} = \mu_{\rm F} + \mu_{\rm B} + E_{\rm b}. \tag{40}$$

Here, $E_{\rm b} = 1/(m a_{\rm BF}^2)$ is the binding energy of a two-body Bose-Fermi bound state. In this regime [$(k_{\rm F}a_{\rm BF})^{-1} \gg 1$], the compressibility matrix $\hat{\kappa}$ in Eq. (17) is parametrized as

$$\hat{\kappa} = \kappa_{\rm CF}\begin{pmatrix} 1 & 1 \\ 1 & 1 \end{pmatrix}, \tag{41}$$

where $\kappa_{\rm CF}$ is diagrammatically given in Fig. 10(b). Equation (41) is consistent with inset (a) in Fig. 9, showing that all the compressibilities $\kappa_{\alpha\beta}$ take almost the same value. We briefly note that a similar "molecular mapping" has also been discussed in the BEC regime of a two-component Fermi gas (where composite molecules are bosons) [76,77].

In Fig. 10(b), $V^{\rm eff}_{\rm CF}$ is an effective intermolecular interaction mediated by virtually dissociated Fermi and Bose atoms, as shown in Fig. 10(c). Similar diagrams have also been discussed as the origin of an effective interaction between Cooper pairs in the BEC regime of a two-component Fermi gas [41,76–79]. In this paper, to analytically sum up the diagrams in Fig. 10(b), we approximate $V^{\rm eff}_{\rm CF}(q, q', \theta_{\boldsymbol{q},\boldsymbol{q}'}, i\omega_n^{\rm F}, i\omega_{n'}^{\rm F})$ in this figure as

$$\left\langle V^{\rm eff}_{\rm CF}\right\rangle = \frac{1}{2}\int d\cos(\theta_{\boldsymbol{q},\boldsymbol{q}'}) V^{\rm eff}_{\rm CF}\left(k_{\rm F}^{\rm CF}, k_{\rm F}^{\rm CF}, \theta_{\boldsymbol{q},\boldsymbol{q}'}, 0, 0\right). \tag{42}$$

In Eq. (42), assuming that the region near the (molecular) Fermi surface is important [80], we fix q and q' the values at the Fermi surface $k_{\rm F}^{\rm CF} = \sqrt{4m\mu_{\rm CF}}$ [81] and take the angular average with respect to the relative angle $\theta_{\boldsymbol{q},\boldsymbol{q}'}$ between $\boldsymbol{q}$ and $\boldsymbol{q}'$ over the Fermi surface. For Matsubara frequencies, we take the analytic continuation $i\omega_n^{\rm F}$, $i\omega_{n'}^{\rm F} \to \omega + i\delta$ and set $\omega = 0$.

These approximations enable us to sum up the diagrams in Fig. 10(b), which gives the RPA-type expression

$$\kappa_{\rm CF} = \frac{\kappa^0_{\rm CF}}{1 + \langle V^{\rm eff}_{\rm CF}\rangle \kappa^0_{\rm CF}}, \tag{43}$$

where

$$\kappa^0_{\rm CF} = \sum_{\boldsymbol{q}} \frac{\partial f_{\rm F}(\xi^{\rm CF}_{\boldsymbol{q}})}{\partial \mu_{\rm CF}} \tag{44}$$

is the compressibility in a free molecular Fermi gas. Evaluation of the averaged interaction $\langle V^{\rm eff}_{{\rm CF}j}\rangle$ gives [82]

$$\langle V^{\rm eff}_{\rm CF}\rangle = \sum_{j=1}^{3} \langle V^{\rm eff}_{{\rm CF}j}\rangle \simeq -\frac{4\pi \times (0.84 a_{\rm BF})}{2m} \quad (<0). \tag{45}$$

Figure 9 shows that $\kappa_{\rm CF}$ in Eq. (43) with the averaged interaction strength $\langle V^{\rm eff}_{{\rm CF}j}\rangle$ in Eq. (45) well describes the SCTMA result for $\kappa_{\rm BB}$.

However, because the second term in Fig. 10(b) has the same diagrammatic structure as $\Delta\kappa_{\rm FF}$ in Fig. 7(a), if the s-wave component unphysically remains in $V^{\rm eff}_{\rm CF}$, it directly affects $\kappa_{\rm CF}$. Indeed, while the s-wave components of $V^{\rm eff}_{\rm CF1}$ and $V^{\rm eff}_{\rm CF2}$ canceled each other out as

$$V^{\rm eff}_{\rm CF1}|_{s\,\rm wave} = -V^{\rm eff}_{\rm CF2}|_{s\,\rm wave} = \frac{4\pi a_{\rm BF}}{2m}, \tag{46}$$

there is no "counter" term to remove the s-wave component of $V^{\rm eff}_{\rm CF3}$ in the SCTMA. In this sense, Pauli's exclusion principle is unphysically broken in $\kappa_{\rm CF}$.

To overcome this problem, we need to go beyond the SCTMA, to include the fourth term $V^{\rm eff}_{\rm CF4}$ in Fig. 10(c) [which plays the same role as $\tilde{V}^{\rm eff}_{\rm FF}$ in Fig. 7(b)]. Then Eq. (45) is replaced by, at $T = 0$,

$$\langle V^{\rm eff}_{\rm CF}\rangle = \sum_{j=1}^{4} \langle V^{\rm eff}_{{\rm CF}j}\rangle \simeq -\frac{4\pi (k^{\rm CF}_{\rm F} a_{\rm BF})^2 \times (0.5 a_{\rm BF})}{2m} \quad (<0). \tag{47}$$

This much weaker interaction than Eq. (45) comes from non-s-wave components. When this improved version is used, the compressibility becomes very close to that in the noninteracting case ($\kappa^0_{\rm CF}$), as shown in Fig. 9. Thus, although the SCTMA can describe the stabilization of the system in the strong-coupling regime due to the formation of Bose-Fermi bound molecules, it again overestimates the magnitude of the molecular compressibility, because of the insufficient treatment of intermolecular interaction.

IV. EFFECTS OF BOSE-BOSE REPULSION $U_{\rm BB}$ ON THE THERMODYNAMIC STABILITY

Because the density collapse discussed in the previous section comes from the effective Bose-Bose attractive interaction mediated by the Fermi component, this singular phenomenon is expected to be suppressed by the direct Bose-Bose repulsion $U_{\rm BB} = 4\pi a_{\rm BB}/m > 0$. Indeed, Fig. 5 confirms this; that is, the collapse temperature $T_{\rm clp}$ decreases with increasing interaction strength $N^{1/3}_{\rm BB} a_{\rm BB}$. In Fig. 5(c), all the compressibilities $\kappa_{\alpha\beta}$,

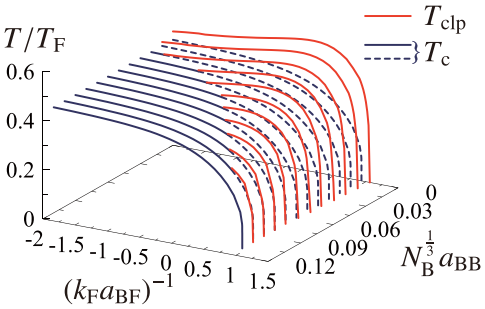

FIG. 11. Calculated collapse temperature $T_{\rm clp}$ in the presence of Bose-Bose repulsion $U_{\rm BB} = 4\pi a_{\rm BB}/m > 0$. When $T_{\rm c} < T_{\rm clp}$ we plot $T_{\rm c}$ with the dashed line.

as well as $\det[\hat{\kappa}]$, are positive everywhere above $T_{\rm c}$, indicating that the system is stabilized by the Bose-Bose repulsion $U_{\rm BB} > 0$. Figure 11 shows $T_{\rm clp}$ and effects of the Bose-Bose repulsion. One sees in this figure that, when $N^{1/3}_{\rm B} a_{\rm BB} \gtrsim 0.11$, one can reach the BEC phase transition without suffering from the density collapse in the whole coupling regime with respect to the heteropairing interaction $(k_{\rm F}a_{\rm BF})^{-1}$.

The previous discussion using Eq. (23) is also applicable to the present case, by replacing the mean-field Bose self-energy in Eq. (24) with

$$\Sigma^{\rm MF}_{\rm B} = \tilde{\Gamma}_{\rm BF} N_{\rm F} + 2U_{\rm BB} N_{\rm B}. \tag{48}$$

Repeating the same discussion as below Eq. (24), one reaches

$$\hat{\kappa}(U_{\rm BB} > 0) = \frac{1}{1 + \left[2U_{\rm BB} - \tilde{\Gamma}^2_{\rm BF}\tilde{\kappa}^0_{\rm FF}\right]\tilde{\kappa}^0_{\rm BB}} \times \begin{pmatrix} \tilde{\kappa}^0_{\rm F} + 2U_{\rm BB}\tilde{\kappa}^0_{\rm FF}\tilde{\kappa}^0_{\rm BB} & -\tilde{\Gamma}_{\rm BF}\tilde{\kappa}^0_{\rm FF}\tilde{\kappa}^0_{\rm BB} \\ -\tilde{\Gamma}_{\rm BF}\tilde{\kappa}^0_{\rm FF}\tilde{\kappa}^0_{\rm BB} & \tilde{\kappa}^0_{\rm BB} \end{pmatrix}. \tag{49}$$

Equation (49) indicates that the compressibility matrix no longer diverges when

$$2U_{\rm BB} - \tilde{\Gamma}_{\rm BF}\tilde{\kappa}^0_{\rm FF} = \frac{8\pi a_{\rm BB}}{m} - \left(\frac{4\pi a_{\rm BF}}{m}\right)^2 \kappa^0_{\rm FF} > 0, \tag{50}$$

which qualitatively explains the behavior of $\kappa_{\alpha\beta}$ in Fig. 5. Comparing the standard RPA expression for the compressibility with $\kappa_{\rm BB}$ in Eq. (49), one finds that the stability condition in Eq. (50) is equivalent to the realization of the situation that the interaction between Bose atoms, $2U_{\rm BB} - \tilde{\Gamma}_{\rm BF}\tilde{\kappa}^0_{\rm FF}$, is repulsive.

While the stabilization of the Bose component is accompanied by the sign change of the Bose-Bose interaction $2U_{\rm BB} - \tilde{\Gamma}_{\rm BF}\tilde{\kappa}^0_{\rm FF}$, the Fermi component becomes stable somehow in a different manner: The (11)-component of Eq. (49) can be written as

$$\kappa_{\rm FF}(U_{\rm BB} > 0) = \frac{\tilde{\kappa}^0_{\rm FF}}{1 - \tilde{\Gamma}^2_{\rm BF}\kappa^{\rm RPA}_{\rm BB}\tilde{\kappa}^0_{\rm FF}}, \tag{51}$$

where

$$\kappa^{\rm RPA}_{\rm BB} = \frac{\tilde{\kappa}^0_{\rm B}}{1 + 2U_{\rm BB}\tilde{\kappa}^0_{\rm B}}. \tag{52}$$

The RPA-type structure in Eq. (51) shows that the effective interaction $-\tilde{\Gamma}^2_{\rm BF}\kappa^{\rm RPA}_{\rm BB}$ between Fermi atoms is always *attractive*, irrespective of the magnitude of $U_{\rm BB} \geqslant 0$. Since $\tilde{\kappa}^0_{\rm BB}$

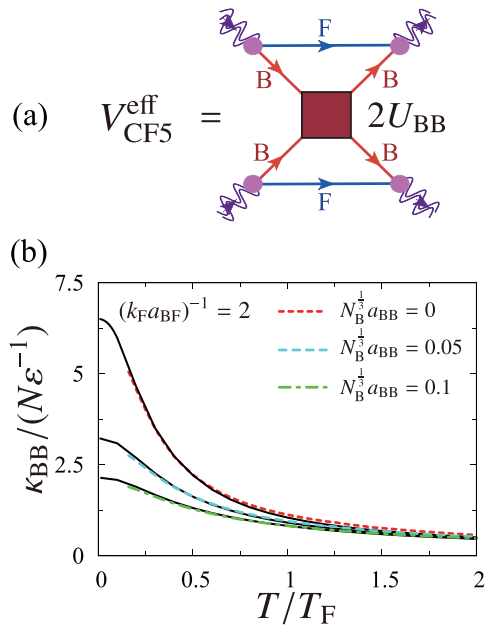

FIG. 12. (a) Additional effective interaction $V^{\rm eff}_{\rm CF5}$ between Fermi molecules in the presence of Bose-Bose repulsion $U_{\rm BB}$. (b) Calculated SCTMA compressibility $\kappa_{\rm BB}$ in the strong-coupling regime when $(k_{\rm F}a_{\rm BF})^{-1} = 2$. Solid lines show $\kappa_{\rm CF}(U_{\rm BB} > 0)$ in Eq. (51). Because the other components $\kappa_{\alpha\beta}$ are almost the same, we only show $\kappa_{\rm BB}$ here.

monotonically increases with decreasing temperature to diverge at the BEC phase transition, the maximum value of $\kappa^{\rm RPA}_{\rm BB}$ in Eq. (52) equals $1/(2U_{\rm BB})$. Thus, even when the stability condition in Eq. (50) is satisfied, the Fermi-Fermi interaction, $-\tilde{\Gamma}^2_{\rm BF}\kappa^{\rm RPA}_{\rm BB}$, is still attractive but is not strong enough to cause the density collapse of the Fermi component.

In the strong-coupling regime where the system is dominated by tightly bound Bose-Fermi molecules, the direct Bose-Bose interaction $U_{\rm BB}$ brings about the additional intermolecular interaction $V^{\rm eff}_{\rm CF5}$ in Fig. 12(a) [83]. Evaluating this diagram as done in Sec. III B, one finds it repulsive, having the form

$$V^{\rm eff}_{\rm CF5} = \frac{8\pi a_{\rm BB}}{m}. \tag{53}$$

Adding this to the averaged interaction $\langle V^{\rm eff}_{\rm CF}\rangle$ in Eq. (45), we see in Fig. 12(b) that the resulting $\kappa_{\rm CF}$ in Eq. (43) agrees well with the SCTMA compressibility in the strong-coupling regime with $U_{\rm BB} > 0$. Thus, the system in this regime is again found to be well described by a weakly interacting molecular Fermi gas, although the present SCTMA overestimates effects of the intermolecular interaction on the compressibility matrix.

V. SUMMARY

To summarize, we have discussed the thermodynamic stability of a Bose-Fermi mixture in the normal state above $T_{\rm c}$. Including strong heteropairing fluctuations associated with a tunable Bose-Fermi attractive interaction $-U_{\rm BF}(< 0)$ within the framework of the SCTMA, as well as a weak Bose-Bose repulsion $U_{\rm BB}(> 0)$ within the mean-field approximation, we calculated the compressibility matrix $\hat{\kappa}$, consisting of $\kappa_{\alpha\beta} = \partial N_\alpha/\partial\mu_\beta$ $(\alpha, \beta = {\rm F}, {\rm B})$. We then determined the collapse temperature $T_{\rm clp}$, below which the system is unstable against density fluctuations, from the weak- to the strong-coupling regime in terms of the Bose-Fermi pairing interaction.

When $U_{\rm BB} = 0$, we showed that $T_{\rm clp}$ is always higher than the BEC phase transition temperature $T_{\rm c}$. All the matrix elements of $\hat{\kappa}$ diverge at $T_{\rm clp}$ and become negative below this temperature, indicating the simultaneous density collapse of both the Bose and the Fermi components. As the origin of this instability, we pointed out an effective Bose-Bose attractive interaction mediated by density fluctuations in the Fermi component. It makes the Bose component unstable, and this singularity is immediately brought to the Fermi component through a Bose-Fermi coupling associated with the heteropairing interaction $-U_{\rm BF}$. We also clarified that this density collapse does not occur when $(k_{\rm F}a_{\rm BF})^{-1} \gtrsim 1.1$. In this strong-coupling regime, most Bose and Fermi atoms form tightly bound Fermi molecules, so that the system properties are close to those of a Fermi gas. Because of this, the bosonic character of a Bose-Fermi mixture, as well as the instability associated with the induced Bose-Bose attraction, is suppressed.

When $U_{\rm BB} > 0$, the collapse temperature $T_{\rm clp}$ is suppressed to eventually disappear when this repulsion is stronger than the Bose-Bose attraction induced by density fluctuations in the Fermi component. In this case, with decreasing temperature, we can reach the BEC phase transition temperature $T_{\rm c}$ without suffering from density collapse.

However, it is still unclear whether the BEC phase is stable down to $T = 0$ or the density collapse occurs at a temperature below $T_{\rm c}$. Because we have only examined the normal state in this paper, extension of the present approach to the BEC phase below $T_{\rm c}$ is an exciting future challenge. In addition, as clarified in this paper, the application of the SCTMA to a Bose-Fermi mixture has room for improvement: In the weak-coupling (strong-coupling) regime with respect to the heteropairing interaction, the calculated Fermi atomic (molecular) compressibility in the SCTMA contradicts with Pauli's exclusion principle, in the sense that it unphysically involves the contribution from the double occupancy of fermions in the same quantum state. Because this deficiency overestimates the Fermi atomic compressibility in the weak-coupling regime, as well as the Fermi molecular compressibility in the strong-coupling regime, how to overcome this problem also remains another future problem. Since the stabilization of a Bose-Fermi mixture with a heteronuclear Feshbach resonance is crucial for study of the strong-coupling properties of this system, as well as for the realization of a stable BEC phase, our results will contribute to the further development of this research field.

ACKNOWLEDGMENTS

We thank D. Kagamihara and R. Sato for discussions. K.M. was supported by the Keio University Doctoral Student Grant-in-Aid Program. Y.O. was supported by a Grant-in-Aid for Scientific Research from MEXT and JSPS in Japan (No. JP18K11345, No. JP18H05406, and No. JP19K03689).

APPENDIX A: STABILITY CONDITIONS FOR A BOSE-FERMI MIXTURE

The thermodynamic stability of the system at fixed Bose and Fermi atomic numbers and temperature is conveniently determined from the Helmholtz free-energy functional [60],

$$F(T, n_\alpha(\boldsymbol{r})) = \int d\boldsymbol{r} \tilde{f}(T, n_\alpha(\boldsymbol{r})), \tag{A1}$$

where $\tilde{f}$ and $n_{\alpha=\mathrm{B,F}}(\boldsymbol{r})$ are the free-energy density and the density distribution in the α component, respectively. When we introduce small density fluctuations $\delta n_\alpha(\boldsymbol{r}) = n_\alpha(\boldsymbol{r}) - N_\alpha/V$ to a uniform system (with the initial density N_α/V) and expand Eq. (A1) with respect to $\delta n_\alpha(\boldsymbol{r})$, the first-order terms are found to vanish due to the particle conservation, $\delta N_\alpha = \int d\boldsymbol{r} \delta n_\alpha(\boldsymbol{r}) = 0$. Retaining terms up to the second order, we have

$$\begin{aligned}\delta^2 F(T, n_\alpha(\boldsymbol{r})) &\equiv F(T, N_\alpha/V + \delta n_\alpha(\boldsymbol{r})) - F(T, N_\alpha/V) \\ &= \frac{1}{2}\int d\boldsymbol{r} (\delta n_\mathrm{F}(\boldsymbol{r}) \quad \delta n_\mathrm{B}(\boldsymbol{r})) \hat{W} \begin{pmatrix} \delta n_\mathrm{F}(\boldsymbol{r}) \\ \delta n_\mathrm{B}(\boldsymbol{r}) \end{pmatrix}.\end{aligned} \tag{A2}$$

Here,

$$\hat{W}(T, N_\alpha/V) = \begin{pmatrix} \dfrac{\partial^2 \tilde{f}}{\partial n_\mathrm{F}^2} & \dfrac{\partial^2 \tilde{f}}{\partial n_\mathrm{B} \partial n_\mathrm{F}} \\ \dfrac{\partial^2 \tilde{f}}{\partial n_\mathrm{F} \partial n_\mathrm{B}} & \dfrac{\partial^2 \tilde{f}}{\partial n_\mathrm{B}^2} \end{pmatrix}_{n_\alpha(\boldsymbol{r}) = N_\alpha/V} \tag{A3}$$

is the Hessian matrix, which determines the thermodynamic stability of a Bose-Fermi mixture [60–62].

The uniform system is stable if and only if the free energy $F(T, N_\alpha/V)$ is minimum ($\delta^2 F < 0$); that is, $\hat{W}$ must be positive definite. Using thermodynamic identities ($\mu_\alpha = \partial F/\partial N_\alpha$), Eq. (A3) can be written as

$$\hat{W}(T, N_\alpha/V) = \begin{pmatrix} \dfrac{\partial \mu_\mathrm{F}}{\partial n_\mathrm{F}} & \dfrac{\partial \mu_\mathrm{F}}{\partial n_\mathrm{B}} \\ \dfrac{\partial \mu_\mathrm{B}}{\partial n_\mathrm{F}} & \dfrac{\partial \mu_\mathrm{B}}{\partial n_\mathrm{B}} \end{pmatrix}_{n_\alpha(\boldsymbol{r}) = N_\alpha/V}, \tag{A4}$$

which just equals the inverse of compressibility matrix $\hat{\kappa}$ in Eq. (15). Substituting $\hat{W} = \hat{\kappa}^{-1}$ into Eq. (A2), we have

$$\delta^2 F = \frac{1}{2}\int d\boldsymbol{r} \left[\frac{\kappa_\mathrm{BB}}{\det[\hat{\kappa}]} \left[\delta n_\mathrm{F}(\boldsymbol{r}) - \frac{\kappa_\mathrm{FB}}{\kappa_\mathrm{BB}} \delta n_\mathrm{B}(\boldsymbol{r}) \right]^2 + \frac{1}{\kappa_\mathrm{BB}} \delta n_\mathrm{B}(\boldsymbol{r})^2 \right]. \tag{A5}$$

Equation (A5) is always positive when $\kappa_\mathrm{BB} > 0$ and $\det[\hat{\kappa}] > 0$, which give the stability conditions in Eq. (16).

In the same manner, Eq. (A5) is always negative when $\kappa_\mathrm{BB} < 0$ and $\det[\hat{\kappa}] > 0$. That is, when the compressibility matrix $\hat{\kappa}$ is negative definite, the system is unstable against density fluctuations $[\delta n_\mathrm{F}(\boldsymbol{r}), \delta n_\mathrm{B}(\boldsymbol{r})]$.

APPENDIX B: ESTIMATION OF N_CF

As given in Eq. (38), deep inside the strong-coupling regime $[(k_\mathrm{F} a_\mathrm{BF})^{-1} \gg 1]$, the particle-particle scattering matrix $\Gamma_\mathrm{BF}(q)$ in Eq. (6) is reduced to the molecular Green's function. Although the simple relation in Eq. (38) is justified only in the strong-coupling limit where the molecular dissociation no longer occurs, $\Gamma_\mathrm{BF}(q)$ in the strong-coupling regime still exhibits a quasipolar structure even away from the strong-coupling limit. Using this similarity, one can conveniently determine the molecular excitation energy $\omega_{\boldsymbol{q}}^\mathrm{CF}$ with momentum $\boldsymbol{q}$ from the (quasi-)pole of the analytic continued particle-particle scattering matrix, within the neglect of the lifetime of molecule, as

$$0 = \frac{m}{4\pi a_\mathrm{BF}} + \mathrm{Re}\left[\Pi_\mathrm{BF}(\boldsymbol{q}, i\omega_n^\mathrm{F} \to \omega_{\boldsymbol{q}}^\mathrm{CF} + i\delta)\right] - \sum_{\boldsymbol{p}} \frac{m}{p^2}. \tag{B1}$$

Here, δ is an infinitesimally small positive number, and we have neglected the imaginary part of $\Pi_\mathrm{BF}(\boldsymbol{q}, i\omega_n^\mathrm{F} \to \omega_{\boldsymbol{q}}^\mathrm{CF} + i\delta)$. Then, simply treating the molecule as a free fermion, we estimate the number N_CF of Fermi molecules as

$$N_\mathrm{CF} = f_\mathrm{F}(\omega_{\boldsymbol{q}}^\mathrm{CF}). \tag{B2}$$

[1] S. Inouye, J. Goldwin, M. L. Olsen, C. Ticknor, J. L. Bohn, and D. S. Jin, Phys. Rev. Lett. **93**, 183201 (2004).

[2] K.-K. Ni, S. Ospelkaus, M. H. G. de Miranda, A. Péer, B. Neyenhuis, J. J. Zirbel, S. Kotochigova, P. S. Julienne, D. S. Jin, and J. Ye, Science **322**, 231 (2008).

[3] I. Bloch, J. Dalibard, and W. Zwerger, Rev. Mod. Phys. **80**, 885 (2008).

[4] J. W. Park, C.-H. Wu, I. Santiago, T. G. Tiecke, S. Will, P. Ahmadi, and M. W. Zwierlein, Phys. Rev. A **85**, 051602(R) (2012).

[5] I. F.-Barbut, M. Delehaye, S. Laurent, A. T. Grier, M. Pierce, B. S. Rem, F. Chevy, and C. Salmon, Science **345**, 1035 (2014).

[6] R. Onofrio, Phys. Usp. **59**, 1129 (2016).

[7] L. D. Macro, G. Valtolina, K. Matsuda, W. G. Tobias, J. P. Covey, and J. Ye, Science **363**, 853 (2019).

[8] C. Chin, R. Grimm, P. Julienne, and E. Tiesinga, Rev. Mod. Phys. **82**, 1225 (2010).

[9] A. Storozhenko, P. Schuck, T. Suzuki, H. Yabu, and J. Dukelsky, Phys. Rev. A **71**, 063617 (2005).

[10] T. Watanabe, T. Suzuki, and P. Schuck, Phys. Rev. A **78**, 033601 (2008).

[11] E. Fratini and P. Pieri, Phys. Rev. A **81**, 051605(R) (2010).

[12] D. Kharga, D. Inotani, R. Hanai, and Y. Ohashi, J. Phys. Soc. Jpn. **86**, 084301 (2017).

[13] K. Manabe, D. Inotani, and Y. Ohashi, Phys. Rev. A **100**, 063609 (2019).

[14] H. Heiselbelg, C. J. Pethick, H. Smith, and L. Viverit, Phys. Rev. Lett. **85**, 2418 (2000).

[15] M. J. Bijlsma, B. A. Heringa, and H. T. C. Stoof, Phys. Rev. A **61**, 053601 (2000).

[16] B. J. DeSalvo, K. Patel, G. Cai, and C. Chin, Nature (London) **568**, 61 (2019).
[17] H. Edri, B. Raz, N. Matzliah, N. Davidson, and R. Ozeri, Phys. Rev. Lett. **124**, 163401 (2020).
[18] D. V. Efremov and L. Viverit, Phys. Rev. B **65**, 134519 (2002).
[19] Z. Wu and G. M. Bruun, Phys. Rev. Lett. **117**, 245302 (2016).
[20] J. J. Kinnunen, Z. Wu, and G. M. Bruun, Phys. Rev. Lett. **121**, 253402 (2018).
[21] D. O. Edwards, D. F. Brewer, P. Seligman, M. Skertic, and M. Yaqub, Phys. Rev. Lett. **15**, 773 (1965).
[22] A. C. Anderson, D. O. Edwards, W. R. Roach, R. E. Sarwinski, and J. C. Wheatley, Phys. Rev. Lett. **17**, 367 (1966).
[23] J. Bardeen, G. Baym, and D. Pines, Phys. Rev. **156**, 207 (1967).
[24] K. Maeda, G. Baym, and T. Hatsuda, Phys. Rev. Lett. **103**, 085301 (2009).
[25] F. P. Laussy, A. V. Kavokin, and I. A. Shelykh, Phys. Rev. Lett. **104**, 106402 (2010).
[26] I. A. Shelykh, T. Taylor, and A. V. Kavokin, Phys. Rev. Lett. **105**, 140402 (2010).
[27] O. Cotlet, S. Zeytinoğlu, M. Sigrist, E. Demler, and A. Imamoğlu, Phys. Rev. B **93**, 054510 (2016).
[28] I. M. Georgescu, S. Ashhab, and F. Nori, Rev. Mod. Phys. **86**, 153 (2014).
[29] G. Modugno, G. Roati, F. Riboli, F. Ferlaino, R. J. Brecha, and M. Inguscio, Science **297**, 2240 (2002).
[30] C. Ospelkaus, S. Ospelkaus, K. Sengstock, and K. Bongs, Phys. Rev. Lett. **96**, 020401 (2006).
[31] S. Ospelkaus, C. Ospelkaus, L. Humbert, K. Sengstock, and K. Bongs, Phys. Rev. Lett. **97**, 120403 (2006).
[32] M. Zaccanti, C. D'Errico, F. Ferlaino, G. Roati, M. Inguscio, and G. Modugno, Phys. Rev. A **74**, 041605(R) (2006).
[33] B. J. DeSalvo, K. Patel, J. Johansen, and C. Chin, Phys. Rev. Lett. **119**, 233401 (2017).
[34] R. S. Lous, I. Fritsche, M. Jag, F. Lehmann, E. Kirilov, B. Huang, and R. Grimm, Phys. Rev. Lett. **120**, 243403 (2018).
[35] See, for example, C. J. Pethick, and H. Smith, *Bose-Einstein Condensation in Dilute Gases* (Cambridge University Press, New York, 2008).
[36] J. M. Gerton, D. Strekalov, I. Prodan, and R. G. Hulet, Nature (London) **408**, 692 (2000).
[37] J. L. Roberts, N. R. Claussen, S. L. Cornish, E. A. Donley, E. A. Cornell, and C. E. Wieman, Phys. Rev. Lett. **86**, 4211 (2001).
[38] E. A. Donley, N. R. Claussen, S. L. Cornish, J. L. Roberts, E. A. Cornell, and C. E. Wieman, Nature (London) **412**, 295 (2001).
[39] C. Eigen, A. L. Gaunt, A. Suleymanzade, N. Navon, Z. Hadzibabic, and R. P. Smith, Phys. Rev. X **6**, 041058 (2016).
[40] Z. Yu and C. J. Pethick, Phys. Rev. A **85**, 063616 (2012).
[41] R. Haussmann, Z. Phys. B: Condens. Matter **91**, 291 (1993).
[42] R. Haussmann, Phys. Rev. B **49**, 12975 (1994).
[43] See, e.g., R. Haussmann, in *Self-consistent Quantum-Field Theory and Bosonization for Strongly Correlated Electron Systems*, Lecture Notes in Physics Vol. 56 (Springer, Berlin, 1999), Chap. 2.
[44] R. Haussmann, W. Rantner, S. Cerrito, and W. Zwerger, Phys. Rev. A **75**, 023610 (2007).
[45] D. M. Eagles, Phys. Rev. **186**, 456 (1969).
[46] A. J. Leggett, in *Modern Trends in the Theory of Condensed Matter*, edited by A. Pekalski and J. Przystawa (Springer-Verlag, Berlin, 1980), p. 14.
[47] P. Nozières and S. Schmitt-Rink, J. Low Temp. Phys. **59**, 195 (1985).
[48] C. A. R. Sá de Melo, M. Randeria, and J. R. Engelbrecht, Phys. Rev. Lett. **71**, 3202 (1993).
[49] Y. Ohashi and A. Griffin, Phys. Rev. Lett. **89**, 130402 (2002).
[50] G. C. Strinati, P. Pieri, G. Röpke, P. Schuck, and M. Urban, Phys. Rep. **738**, 1 (2018).
[51] Y. Ohashi, H. Tajima, and P. van Wyk, Prog. Part. Nucl. Phys. **111**, 103739 (2020).
[52] C. A. Regal, M. Greiner, and D. S. Jin, Phys. Rev. Lett. **92**, 040403 (2004).
[53] M. W. Zwierlein, C. A. Stan, C. H. Schunck, S. M. F. Raupach, A. J. Kerman, and W. Ketterle, Phys. Rev. Lett. **92**, 120403 (2004).
[54] J. Kinast, S. L. Hemmer, M. E. Gehm, A. Turlapov, and J. E. Thomas, Phys. Rev. Lett. **92**, 150402 (2004).
[55] M. Bartenstein, A. Altmeyer, S. Riedl, S. Jochim, C. Chin, J. H. Denschlag, and R. Grimm, Phys. Rev. Lett. **92**, 203201 (2004).
[56] K. Mølmer, Phys. Rev. Lett. **80**, 1804 (1998).
[57] T. Miyakawa, T. Suzuki, and H. Yabu, Phys. Rev. A **64**, 033611 (2001).
[58] R. Roth, Phys. Rev. A **66**, 013614 (2002).
[59] M. Modugno, F. Ferlaino, F. Riboli, G. Roati, G. Modugno, and M. Inguscio, Phys. Rev. A **68**, 043626 (2003).
[60] L. Viverit, C. J. Pethick, and H. Smith, Phys. Rev. A **61**, 053605 (2000).
[61] K. Shirasaki, E. Nakano, and H. Yabu, Phys. Rev. A **90**, 063629 (2014).
[62] Z.-Q. Yu, S. Zhang, and H. Zhai, Phys. Rev. A **83**, 041603(R) (2011).
[63] In this simplified notation, while p has the boson Matsubara frequency (Bose type) in $G_{\rm B}(p)$ and $\Sigma_{\rm B}(p)$, it has the fermion Matsubara frequency (Fermi type) in $G_{\rm F}(p)$, $\Sigma_{\rm F}$, and $\Gamma_{\rm BF}(p)$, as well as $\Pi_{\rm BF}(p)$. For the 2×2 matrix $\Lambda(p)$ in Eq. (18), p in the (11)-component is the Fermi type and p in the (22)-component is the Bose type. The types of variables p and p' in $\hat{T}_0$ in Eq. (20) also depend on whether they appear in $G_{\rm B}$ or $G_{\rm F}$.
[64] J. M. Luttinger and J. C. Ward, Phys. Rev. **118**, 1417 (1960).
[65] G. Baym and L. P. Kadanoff, Phys. Rev. **124**, 287 (1961).
[66] G. Baym, Phys. Rev. **127**, 1391 (1962).
[67] A. Guidini, G. Bertaina, E. Fratini, and P. Pieri, Phys. Rev. A **89**, 023634 (2014).
[68] N. M. Hugenholtz and D. Pines, Phys. Rev. **116**, 489 (1959).
[69] K. Seo and C. A. R. Sá de Melo, arXiv:1105.4365.
[70] H. Bethe and E. Salpeter, Phys. Rev. **84**, 1232 (1951).
[71] K. Maki, Prog. Theor. Phys. **40**, 193 (1968).
[72] R. S. Thompson, Phys. Rev. B **1**, 327 (1970).
[73] D. Kagamihara, D. Inotani, and Y. Ohashi, J. Phys. Soc. Jpn. **88**, 114001 (2019).
[74] L. G. Aslamazov and A. I. Larkin, Phys. Lett. A **26**, 238 (1968).
[75] See, e.g., *Theoretical Methods for Strongly Correlated Electrons*, edited by D. Sénécal, A.-M. S. Tremblay, and C. Bourbonnais (Springer, New York, 2004).
[76] R. Sato, D. Kagamihara, K. Manabe, H. Tajima, D. Inotani, and Y. Ohashi (unpublished) (2021).
[77] G. C. Strinati, P. Pieri, and C. Lucheroni, Eur. Phys. J. B **30**, 161 (2002).
[78] P. Pieri and G. C. Strinati, Phys. Rev. B **61**, 15370 (2000).
[79] M. Pini, P. Pieri, and G. C. Strinati, Phys. Rev. B **99**, 094502 (2019).

[80] A. A. Abrikosov, L. P. Gorkov, and I. E. Dzyaloshinski, *Methods of Quantum Field Theory in Statistical Physics* (Dover, Mineola, NY, 1975).

[81] In the high-temperature region where $\mu_{\rm CF} < 0$, we take $k_{\rm F}^{\rm CF} = 0$.

[82] In computing $\langle V_{\rm CF3}^{\rm eff} \rangle$, we approximated the dressed Green's functions G_α to the bare ones G_α^0. We then analytically summed up the Matstubara frequencies, by expanding $V_{\rm CF3}^{\rm eff}$ with respect to the Bose and Fermi fugacities to the leading order. The resulting expression involves the sum of the Bose and Fermi chemical potentials, which we evaluated by using Eq. (40) as $\mu_{\rm F} + \mu_{\rm B} = \mu_{\rm CF} - E_{\rm b}$. Here, we determined $\mu_{\rm CF}$ from the number equation of a free molecular Fermi gas.

[83] M. Yu. Kagan, I. V. Brodsky, D. V. Efremov, and A. V. Klaptsov, Phys. Rev. A **70**, 023607 (2004).